

Primordial black holes and gravitational waves in non-standard cosmologies

Sukannya Bhattacharya,^a Subhendra Mohanty,^a Priyank Parashari^{a,b}

^aTheoretical Physics Division, Physical Research Laboratory, Navrangpura, Ahmedabad - 380009, India.

^bIndian Institute of Technology, Gandhinagar, 382355, India

E-mail: sukannya@prl.res.in, mohanty@prl.res.in, parashari@prl.res.in

Abstract. For primordial black holes (PBH) to form a considerable fraction of cold dark matter, the required amplitude of primordial scalar perturbations is quite large ($P_\zeta(k) \sim 10^{-2}$) if PBH is formed in radiation epoch. In alternate cosmological histories, where additional epochs of arbitrary equation of state precede radiation epoch, the dynamics of PBH formation and relevant mass ranges can be different leading to requirement of lower primordial power at smaller scales of inflation. Moreover, this alternate history can modify the predictions for the gravitational wave (GW) spectrum, which can be probed by upcoming GW observations. In this paper we show that an early kination epoch can lead to percent level abundance of PBH for a lower amplitude of $P_\zeta(k)$ as compared to PBH formation in a standard radiation epoch. Moreover, we calculate the effect of early kination epoch on the GW spectrum for first and second orders in perturbation which show enhancement in the amplitude of the GW spectrum in a kination epoch with respect to that in a standard radiation epoch.

Contents

1	Introduction	1
2	Pre-radiation epoch of stiff domination	3
3	Formation of PBH	4
4	Analysis for different primordial power spectra	7
4.1	Scale invariant power spectrum	7
4.2	Broken power law power spectrum	9
4.3	Gaussian power spectrum	9
5	Modification of the Gravitational Wave spectra	10
5.1	First order perturbation theory	11
5.2	Second order perturbation theory	12
5.2.1	Tensor Transfer Function	14
5.2.2	Second order GW spectrum for Gaussian Power spectrum	15
5.2.3	Second order GW spectrum for Broken Power spectrum	16
6	Discussion and summary	16
A	Transfer function for first-order scalar modes	22

1 Introduction

The phenomenology of the early universe has entered a phase more rich than ever considering the numerous theoretical models in literature as well as the huge influx of data from several present and upcoming observations. The inflationary epoch, predicting quasi-exponential expansion for ~ 55 e-folds before hot big bang expansion, is constrained by the Cosmic Microwave Background (CMB) surveys (latest is Planck 2018 [1, 2]), which predict the power spectrum of the primordial scalar fluctuations to be slightly red-tilted. However, CMB only probes $10 - 15$ e-folds around the pivot scale $k_{\text{pivot}}^{\text{CMB}} = 0.002 \text{ Mpc}^{-1}$. Lack of direct probe for the remaining ~ 40 e-folds leaves room for exploration where some models of inflation may have non-standard predictions. A possible deviation from the red-tilt of the scalar power spectrum can take place for these smaller scales of inflation, which can lead to a rise in the scalar power spectrum. When these scales re-enter the horizon, the large density fluctuations may collapse gravitationally to form primordial black holes (PBH).

PBH are non-relativistic and effectively collisionless and therefore have been proposed to be a dark matter (DM) candidate in early literature [3–5]. PBH as a candidate for DM has regained attention after the first detection of gravitational waves (GW) by Advanced LIGO/VIRGO in 2017 [6–12]. These GW interferometers have since detected several binary black hole mergers with mass of the initial components ranging from $8 - 40M_{\odot}$. Stellar black holes, which form at the end points of stellar evolution under gravitational collapse after a supernova explosion, rarely have mass $\geq 10M_{\odot}$ as constrained from the X-ray emission from their accretion disks. Moreover, given the high merging rates inferred by LIGO/VIRGO and

the observed low effective spin point towards the possibility that the detected massive BH are of primordial origin.

Although solar mass black holes are interesting given the detections of GW interferometers till date, the range of possible PBH mass M and their abundance $f_{\text{PBH}}(M)$ is constrained from many cosmological and astrophysical observations [13]. Due to Hawking radiation, PBHs evaporate on a time scale $t_{\text{ev}} = \frac{5120\pi G^2 M^3}{\hbar c^4}$, so that PBHs of mass lower than $\sim 10^{15}$ gm have completely evaporated by now. PBHs of mass $M \sim 10^{16}$ gm are on the verge of complete evaporation and thus have remnants from their Hawking evaporation in the extragalactic photon background, which is constrained with experiments such as Fermi Large Area Telescope [13]. Lack of femtolensing detection in Fermi experiment [14] signifies that PBHs of mass $M \sim 5 \times 10^{17} - 10^{20}$ gm cannot contribute to a large fraction whereas lack of microlensing events in EROS survey [15] and MACHO collaboration [16] constrain the abundance of PBH in the mass range $M \sim 10^{26} - 10^{33}$ gm. For massive PBHs, X-ray emission near PBH due to accretion of gas may modify recombination history and therefore affect spectral distortions and temperature anisotropies in CMB which constrain the abundance of PBHs with solar mass and above [17, 18]. However, considering late time merging of PBHs, sub-solar mass PBHs can give rise to solar and super-solar mass PBHs that are observed now. Considering all these bounds, there is a very small range of masses $M \sim 10^{20} - 10^{23}$ gm with feeble constraints from microlensing experiments such as Subaru HSC [19], where PBH can still constitute the totality of DM.

PBH formation during radiation domination requires a large amplitude of the primordial curvature perturbation $P_\zeta(k) \simeq 0.02$, much larger than $P_\zeta(k) = 2.1 \times 10^{-9}$ constrained by CMB observations [2] at CMB relevant scales. Numerous studies have been done inspecting possible rise in power at smaller scales $k > k_{\text{CMB}}$ for several theoretically and phenomenologically motivated models of inflation [20–32, 43, 45]. For single field slow roll models of inflation, it is hard to achieve an ultra slow-roll ($\epsilon \sim 10^{-7}$) for smaller scales necessary for large power which is sometimes achieved by including an inflection point in the inflaton potential. For multi-field models of inflation and warm inflation it is possible to achieve large power in the last 40 e-folds of inflation involving the dynamics of fields other than inflation. However, if PBH is formed in a pre-BBN epoch where the effective equation of state is different from $1/3$, then the critical density contrast and the background evolution are different which leads to a modification in the resulting PBH abundance. [33–38] analyse formation of PBH in an early matter dominated epoch whereas [32] explore PBH formation during reheating. However, in alternate cosmological histories where a non-standard epoch precedes radiation epoch before BBN, the effective equation of state can even be $1/3 < w < 1$. In this paper, we consider formation of PBH in such a non-standard pre-BBN epoch and analyse the resulting PBH abundance.

During inflation, the quantum fluctuations of inflaton and metric perturbations result in fluctuations at all scales. Scalar, vector and tensor fluctuations evolve independent of each other in the first order of perturbation theory, however their evolutions are coupled when one considers second and higher order perturbations. The primordial tensor power spectrum at the first order is almost scale-independent with very small amplitude and the resulting gravitational waves (GW) energy density Ω_{GW} following a standard post-inflationary evolution until now is beyond the reach of the sensitivities of current GW observations. But, the large curvature power spectra at small scales of inflation may give rise to large amplitude of tensor power spectrum at the second order leading to large Ω_{GW} at high frequencies $f = ck/2\pi$, which can be within the sensitivity range proposed by the upcoming GW surveys such

as Pulsar Time Arrays (PTA), LISA and DECIGO [39–42]. [44] has explored second order GW spectra for several forms of primordial curvature power spectra with large amplitudes at small scales, which lead to PBH formation in radiation epoch. Here we analyse the effect of a non-standard pre-BBN epoch on first and second order GW spectra given large amplitude of primordial curvature power spectrum at small scales (high frequencies).

In this paper, we show the predictions for PBH and GW in an alternate cosmological history where a kination epoch ($w = 1$) takes place between end of inflation and onset of radiation.¹ The relevant quantities are derived in terms of a general w in the range $1/3 < w < 1$ throughout, but the final results are shown only for $w = 1$ for clarity and simplicity. The rest of this paper is organized as follows. In Sec. 2 we discuss the evolution of the energy density in the presence of a non-standard pre-BBN epoch. In Sec. 3 we derive the formation mechanism of PBH in such a non-standard epoch and compare the resulting abundance to PBH formation in a radiation epoch. In Sec. 4, we consider different primordial curvature power spectra to arrive at an exact result for the PBH mass spectrum and abundance formed in an early kination epoch and we compare the results to those in radiation epoch resulting from the same set of power spectra. In Sec. 5, we have derived the GW spectrum for the modified pre-BBN evolution. In Subsection 5.1, the enhancement first order GW spectrum is shown as a function of the scale of inflation H_{inf} and in Subsection 5.2, the second order GW spectrum is derived for an early kination epoch. In Sec. 6, discuss our results, conclude and comment on the possible future directions.

2 Pre-radiation epoch of stiff domination

The observed abundance of light elements predicts that Big Bang Nucleosynthesis (BBN) must have taken place during radiation domination at $T_{\text{BBN}} \simeq 1\text{MeV}$ and the evolution before that $T > T_{\text{BBN}}$ remains inaccessible to direct observational techniques. Assuming instant reheating of the universe after inflation, the post-inflationary pre-BBN epoch is considered to be radiation dominated in the standard big bang evolution. The simplest deviation from this scenario involves a reheating process where the inflaton field oscillates around the minimum of the potential for a few e-folds with an average equation of state $0 < w < 1/3$ (for $V(\phi) \propto \phi^p$ with $p \leq 4$). Many models of inflation predict additional epochs after reheating when an additional scalar field in the theory, which was inactive during inflation, dominates with an effectively matter-like equation of state ($w = 0$) and decays, such as moduli domination at the end of several string theory inspired models of inflation. However, in general there can be a post-inflationary epoch with a stiff equation of state $1/3 < w < 1$ which dominates the energy density before the onset of radiation domination [46]. Such a stiff dominated (SD) epoch may arise when a sterile field enters the post-inflationary phase with dominant energy density that falls faster than radiation energy density with time. A particular well-studied example are quintessence models of inflation [48, 49] where the post-inflationary epoch is dominated by the inflaton’s kinetic energy with equation of state $w \approx 1$ before transition into the radiation epoch sometime before BBN. As the universe expands, a smooth transition from such an early kination epoch ($\rho \sim a^{-6}$) to radiation domination ($\rho \sim a^{-4}$) takes place at temperature T_1 .

¹Here, we do not refer to the kinetic energy domination by slow roll violation at the end of inflation, since this is a very short phase and any PBH produced in this epoch will be of microscopic mass, therefore irrelevant to us.

We consider a stiff dominated epoch with a constant equation of state w which dominates the energy density of the universe from the end of inflation until the onset of radiation at temperature T_1 . We assume instantaneous transition from SD to radiation domination at T_1 . The energy density at any time during this SD epoch is given in terms of the temperature at that time:

$$\rho_{\text{SD}}(T) = \rho(T) = \rho_{\text{SD}}(T_1) \left(\frac{a(T_1)}{a(T)} \right)^{3(1+w)}. \quad (2.1)$$

And the energy density of SD and radiation can be equated at the transition such that:

$$\rho_{\text{SD}}(T_1) = \rho_{\text{rad}}(T_1) = \frac{\pi^2}{30} g_*(T_1) T_1^4, \quad (2.2)$$

where g_* signifies the number of degrees of freedom. Moreover, conservation of entropy provides:

$$\frac{a(T_1)}{a(T)} = \left(\frac{g_s(T)}{g_s(T_1)} \right)^{1/3} \frac{T}{T_1}, \quad (2.3)$$

where g_s is the entropy number of degrees of freedom. Therefore,

$$\rho_{\text{SD}}(T) = \frac{\pi^2}{30} g_*(T_1) \left(\frac{g_s(T)}{g_s(T_1)} \right)^{1+w} \left(\frac{T}{T_1} \right)^{3(1+w)} T_1^4. \quad (2.4)$$

Evidently, this epoch has the maximum energy density at $T = T_{\text{reh}}$ (or $T = T_{\text{infl.end}}$ for an instantaneous reheating) and minimum possible energy density at $T_1 = T_{\text{BBN}} \simeq 1\text{MeV}$ equal to the radiation energy density at T_1 .

If PBH formation takes place in such a SD epoch with $1/3 < w < 1$, then the modified background evolution can affect the abundance of PBH corresponding to the modes entering the horizon in this epoch. The evolution of the source-free first order tensor power spectrum is different in a SD epoch as compared to radiation epoch [47] and can have an effective w -dependent blue-tilt. Moreover, the large amplitude of the primordial curvature power spectrum can source a large tensor power spectrum when second and higher order perturbation theory is considered. The resulting tensor power spectrum will evolve differently in a pure radiation epoch after inflation and in such an alternate cosmological history leading to different $\Omega_{\text{GW}}^0 h^2$ that can be probed by future GW interferometers.

In rest of this paper, we present the calculations and basic notions for PBH formation dynamics and GW spectrum in terms of a general stiff epoch with equation of state (e.o.s.) w , however, for the sake of clarity, while showing final results and plots, we resort particularly to an early kination epoch, $w = 1$.

3 Formation of PBH

PBH can be formed in the early universe when the density fluctuations of high amplitude re-enter the Hubble horizon at post-inflationary epochs and collapse gravitationally below the Schwarzschild radius. The mass of the PBH at formation is:

$$M = \gamma M_H = \gamma \frac{4}{3} \pi (H^{-1})^3 \rho, \quad (3.1)$$

where M_H is the horizon mass, γ describes the efficiency of the gravitational collapse [5] and H is the Hubble parameter at formation. PBH formation in the radiation epoch is

studied in great detail in literature². However, as discussed in the introduction, the critical density contrast in radiation domination is such that the amplitude of primordial scalar power necessary for PBH production during radiation epoch is $\sim 10^{-2}$. In this section, we analyze the energy budget of PBHs formed during a stiff epoch with arbitrary $1/3 < w < 1$ and analyze if considerable PBH abundance can be achieved with a lower amplitude of primordial scalar power.

The Friedmann equation for a stiff epoch can be written as : $H^2 = 8\pi\rho_{\text{SD}}(T)/3$ in $M_{\text{Pl}} = 1$ units. For a PBH formed in this epoch, the mass at formaion is:

$$M(T) = \frac{\gamma}{2GH} = \frac{\gamma}{2G} \sqrt{\frac{3}{8\pi G}} \frac{1}{\sqrt{\rho_{\text{SD}}(T)}} = \left(\frac{\gamma}{2G}\right) \left(\frac{\pi^2 g_*(T_1)}{30} \times \frac{8\pi G}{3}\right)^{-\frac{1}{2}} \left(\frac{g_s(T_1)}{g_s(T)}\right)^{\frac{1+w}{2}} \left(\frac{T_1}{T}\right)^{\frac{3(1+w)}{2}} \frac{1}{T_1^2}. \quad (3.2)$$

The mass of a PBH formed in this epoch can be expressed in terms of the wavenumber k of the fluctuations that entered the horizon³ at temperature T . The Hubble parameter can be written as:

$$\frac{H(T)}{H_{\text{eq}}} = \frac{H(T)}{H(T_1)} \frac{H(T_1)}{H_{\text{eq}}} = \left(\frac{a(T_1)}{a(T)}\right)^{\frac{3(1+w)}{2}} \left(\frac{a_{\text{eq}}}{a(T_1)}\right)^2, \quad (3.3)$$

where H_{eq} is the Hubble parameter at T_{eq} . Therefore, combining Eq. (3.1) and Eq. (3.3), the mass of PBH corresponding to mode k is:

$$M(k) = \left(\frac{\gamma}{2G}\right) \left(\frac{\pi^2 g_*^{\text{eq}}}{15} \times \frac{8\pi G}{3}\right)^{\frac{1}{3w+1}} \left(\frac{g_s^{\text{eq}}}{g_s(T_1)}\right)^{\frac{3w-1}{3(3w+1)}} (a_{\text{eq}} T_{\text{eq}})^{\frac{3(1+w)}{3w+1}} T_1^{-\frac{3w-1}{3w+1}} k^{-\frac{3(1+w)}{3w+1}}. \quad (3.4)$$

Now, the abundance of PBHs of mass M over the logarithmic interval $d \ln M$ can be estimated as:

$$f_{\text{PBH}}(M) \equiv \frac{\Omega_{\text{PBH}}(M)}{\Omega_c}, \quad (3.5)$$

where $\Omega_{\text{PBH}}(M)$ is the density contribution of PBHs of mass M of the total contribution Ω_c from cold dark matter. So, $f_{\text{PBH}}(M) = 1$ means that PBHs with a monochromatic mass distribution of mass M constitute all of the cold dark matter. For a general mass distribution, $f_{\text{PBH}}(M)$ can be determined neglecting the accretion and evaporation of the PBHs. Thus, for PBHs formed in a post-reheating SD epoch of our consideration, the abundance will depend on the fractional contribution of PBHs at the end of that epoch, i.e., $\rho_{\text{PBH}}(M)|_{T_1}$. The fraction of the universe collapsing into black holes of masses between M and $M + d \ln M$ can be estimated in the Press-Schechter model of gravitational collapse as:

$$\beta(M) \equiv \frac{1}{\rho_{\text{tot}}} \frac{d\rho_{\text{PBH}}(M)}{d \ln M} = 2 \int_{\zeta_c}^{\infty} \frac{1}{\sqrt{2\pi}\sigma(M)} e^{-\frac{\zeta^2}{2\sigma(M)^2}} d\zeta = \text{erfc}\left(\frac{\zeta_c}{\sqrt{2}\sigma(M)}\right). \quad (3.6)$$

Here, $\zeta_c = \frac{(5+3w)}{2(1+w)}\delta_c$, where δ_c the critical density contrast of perturbations to gravitationally collapse and form PBH.

$\sigma(M)$ is the variance of curvature fluctuations and is related to the primordial fluctuations through an window function $W(k, R)$. Generally $W(k, R)$ is considered to be simple top hat function centered at k_{PBH} over which the power spectrum $P_{\zeta}(k)$ varies linearly [50].

²See references in the 4th paragraph in Sec. 1 and the references therein.

³Throughout the manuscript, we consider that perturbations at mode $k = aH$ collapses immediately after entering horizon.

The dependence of the critical density contrast on the equation of state has been studied analytically [5] and numerically [51] and we will consider the more precise numerical form [51]⁴

$$\delta_c = \frac{3(1+w)}{(5+3w)} \sin^2 \left(\frac{\pi\sqrt{w}}{(1+3w)} \right). \quad (3.7)$$

Considering $\sigma^2(M) = P_\zeta(k)$, the function $\beta(M)$ can be written explicitly in terms of curvature perturbation spectrum $P_\zeta(k)$ as:

$$\beta(M) = \operatorname{erfc} \left[\frac{3 \times \sin^2 \left(\frac{\pi\sqrt{w}}{(1+3w)} \right)}{2\sqrt{2P_\zeta(k)}} \right]. \quad (3.8)$$

After formation, ρ_{PBH} grows as matter (a^3), whereas the background energy density grows as $\sim a^{-3(1+w)}$ until the temperature reaches T_1 and then as $\sim a^4$ until matter-radiation equality at T_{eq} . Moreover, at the time of formation (PBH of mass M is formed at temperature T), only a fraction $\gamma\beta(M)$ of the total energy density turns into PBH. Therefore, considering all these factors,

$$\begin{aligned} f_{\text{PBH}}(M) &= \frac{\Omega_{\text{PBH}}(M)}{\Omega_c} = \frac{\rho_{\text{PBH}}(M)}{\rho_c} \Big|_{\text{eq}} \\ &= \frac{\rho_{\text{PBH}}(M)}{\rho_{\text{rad}}} \Big|_{\text{eq}} \left(\frac{\Omega_m h^2}{\Omega_c h^2} \right) \\ &= \frac{\rho_{\text{PBH}}(M)}{\rho_{\phi_1}} \Big|_{T_1} \left(\frac{a(T_{\text{eq}})}{a(T_1)} \right) \left(\frac{\Omega_m h^2}{\Omega_c h^2} \right) \\ &= \frac{\rho_{\text{PBH}}(M)}{\rho_{\phi_1}} \Big|_T \left(\frac{a(T_1)}{a(T)} \right)^{3w} \left(\frac{a(T_{\text{eq}})}{a(T_1)} \right) \left(\frac{\Omega_m h^2}{\Omega_c h^2} \right). \end{aligned} \quad (3.9)$$

Here, in the second line we have used the condition that matter and radiation energy density are equal at T_{eq} . Similarly, in the third line, we have used $\rho_{\phi_1}(T_1) = \rho_{\text{rad}}(T_1)$. Using the conservation of entropy density at T_{eq} , T_1 and T ,

$$a(T_{\text{eq}})^3 T_{\text{eq}}^3 g_s(T_{\text{eq}}) = a(T_1)^3 T_1^3 g_s(T_1) = a(T)^3 T^3 g_s(T), \quad (3.10)$$

Eq. (3.9) can be written in terms of temperature T of PBH formation as:

$$f_{\text{PBH}}(M) = \gamma\beta(M) \left(\frac{g_s(T)}{g_s(T_1)} \right)^w \left(\frac{g_s(T_1)}{g_s(T_{\text{eq}})} \right) \left(\frac{T}{T_1} \right)^{3w} \left(\frac{T_1}{T_{\text{eq}}} \right) \left(\frac{\Omega_m h^2}{\Omega_c h^2} \right). \quad (3.11)$$

Substituting T from Eq. (3.2) in Eq. (3.11), the abundance can be expressed in terms of M as:

$$f_{\text{PBH}}(M) = \frac{\gamma}{T_{\text{eq}}} \left(\frac{g_s(T_1)}{g_s(T_{\text{eq}})} \right)^{1/3} \left(\frac{\Omega_m h^2}{\Omega_c h^2} \right) \left(\frac{3}{8\pi G} \frac{30}{\pi^2 g_*} \right)^{\frac{w}{1+w}} \left(\frac{\gamma}{2G} \right)^{\frac{2w}{1+w}} T_1^{\frac{1-3w}{1+w}} \beta(M) M^{-\frac{2w}{1+w}}. \quad (3.12)$$

⁴This expression for δ_c fails in a matter dominated epoch where it predicts the critical density contrast to be $\simeq 0$ such that all possible density perturbations entering the horizon can collapse [52]. But, one can consider Eq. (3.7) to be valid in a range $0 \ll w < 1$ which is a superset of the SD equation of state considered here.

Therefore, for an extended mass distribution, the total abundance of PBH is:

$$f_{\text{PBH}}^{\text{tot}} = \int f_{\text{PBH}}(M) d \ln M = \mathcal{C}_1 \times \mathcal{C}_2(w) \times T_1^{\frac{1-3w}{1+w}} \int \beta(M) M^{-\frac{2w}{1+w}} d \ln M, \quad (3.13)$$

where

$$\mathcal{C}_1 = \frac{\gamma}{T_{\text{eq}}} \left(\frac{g_s(T_1)}{g_s(T_{\text{eq}})} \right)^{1/3} \left(\frac{\Omega_m h^2}{\Omega_c h^2} \right) \text{ and } \mathcal{C}_2(w) = \left(\frac{3}{8\pi G} \frac{30}{\pi^2 g_*} \left(\frac{\gamma}{2G} \right)^2 \right)^{\frac{w}{1+w}}. \quad (3.14)$$

Eq. (3.11) can express the abundance of PBHs of mass M produced in a radiation epoch with the limit $w \rightarrow 1/3$ and $T_1 \rightarrow T_{\text{eq}}$, so that,

$$f_{\text{PBH}}^{\text{rad}}(M) = \gamma \beta^{\text{rad}}(M) \left(\frac{g_s(T)}{g_s(T_{\text{eq}})} \right)^{1/3} \left(\frac{T}{T_{\text{eq}}} \right) \left(\frac{\Omega_m h^2}{\Omega_c h^2} \right), \quad (3.15)$$

where $\beta^{\text{rad}}(M) = \text{erfc} \left(\frac{1.02}{\sqrt{2P_\zeta(k)}} \right)$, since $\zeta_c = 1.02$ in a radiation dominated epoch. Thus, for any given primordial power $P_\zeta(k)$, the gain in the abundance of PBH in a stiff dominated epoch over a radiation dominated epoch is:

$$g_f = \frac{f_{\text{PBH}}(M)}{f_{\text{PBH}}^{\text{rad}}(M)} = \frac{\beta(M)}{\beta^{\text{rad}}(M)} [g_s(T)]^{w-1/3} [g_s(T_1)]^{1-w} [g_s(T_{\text{eq}})]^{-2/3} \left(\frac{T}{T_1} \right)^{3w-1}. \quad (3.16)$$

For all $1/3 < w < 1$, we find $g_f > 1$ even for an instantaneous SD, i.e., $T \simeq T_1$. Therefore, a lower amplitude of the curvature power spectrum than that required for PBH formation in radiation epoch can lead to a considerable percent level PBH abundance for a PBH formation in SD epoch.

4 Analysis for different primordial power spectra

In this section, we study three different types of primordial curvature power spectra from a phenomenological approach from similar motivations as [44]. Apart from the first case, which provides a clear idea about requirement of smaller power in a SD epoch, other two cases are motivated by theories of inflation.

4.1 Scale invariant power spectrum

Here, we consider a constant amplitude of the primordial curvature power spectrum for all modes beyond k_p such that:

$$P_\zeta(k) = A_s \left(\frac{k}{k_*} \right)^{n_s-1} + P_p \Theta(k - k_p), \quad (4.1)$$

where P_p is the power at all scales with $k > k_p$. We emphasize that such a constant amplitude of the scalar power at small scales is not motivated by theoretical considerations and eventually leads to a considerable abundance of PBH for all the masses below $M(k_p)$, however, we show the results for this case for simplicity and completion.

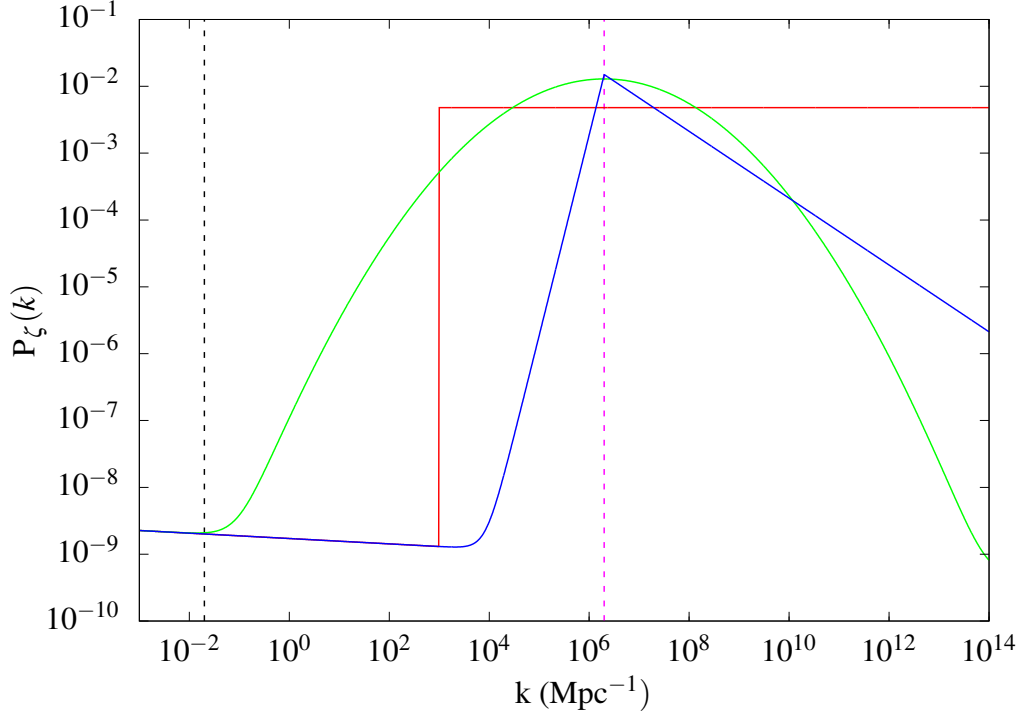


Figure 1. Curvature power spectrum for different cases: *Red*: Scale invariant, *Blue*: Broken power law, *Green*: Gaussian power spectrum. Black dashed line points to the CMB pivot scale $k_{\text{pivot}}^{\text{CMB}} = 0.002 \text{ Mpc}^{-1}$ and magenta dashed line signifies $k_p = 2 \times 10^6 \text{ Mpc}^{-1}$ for production of solar mass PBH.

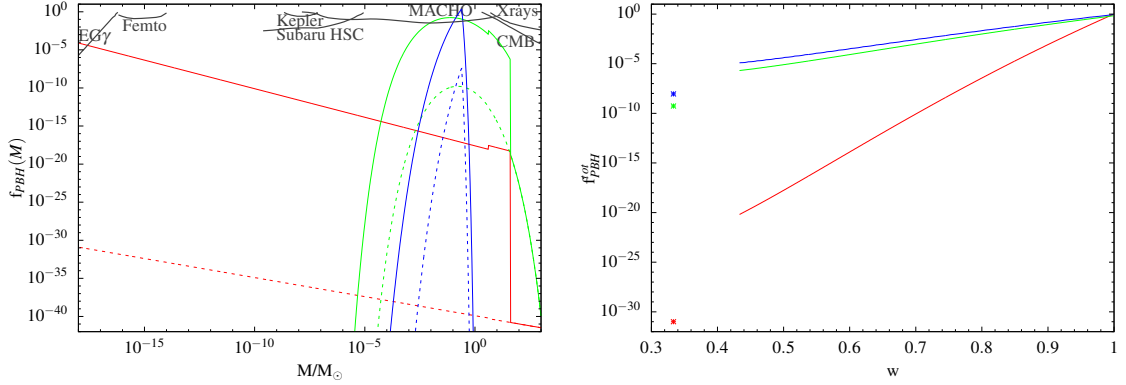


Figure 2. *Left panel*: Abundance of PBH for scale invariant power spectrum (red), for broken power law power spectrum (blue) and for gaussian power spectrum (green) for PBH formation in a pure radiation dominated epoch (dashed lines) and in a kination epoch before radiation domination (solid lines). Constraints on the PBH mass spectrum from different astrophysical and cosmological observations are shown in grey lines. *Right panel*: Total abundance of PBH (solid lines) as a function of equation of state w of an arbitrary epoch of scalar domination before radiation epoch, whereas crosses mark total abundance for PBH formation in a pure radiation epoch for the three different types of power spectra. The peak scale considered is $k_p = 2 \times 10^6 \text{ Mpc}^{-1}$ to have considerable amount of solar mass PBH.

4.2 Broken power law power spectrum

In various scenarios where PBH is produced from domain walls or vacuum bubbles [53], the relevant primordial curvature power spectrum has a broken power law expansion such as:

$$P_\zeta(k) = A_s \left(\frac{k}{k_*} \right)^{n_s-1} + P_p \left(\frac{k}{k_p} \right)^m \quad k < k_p, \quad (4.2)$$

$$= A_s \left(\frac{k}{k_*} \right)^{n_s-1} + P_p \left(\frac{k}{k_p} \right)^{-n} \quad k \geq k_p. \quad (4.3)$$

We consider the case where $m = 3$ and $n = 0.5$.

4.3 Gaussian power spectrum

In many models of smooth waterfall hybrid inflation [43] and several inflection point models of inflation [45], the potential features a plateau for a few e-folds before the end of inflation. This plateau regime of the potential can lead to a peak in the curvature power spectrum which, at the simplest approach, can be written as a Gaussian power spectrum of the following form:

$$P_\zeta(k) = A_s \left(\frac{k}{k_*} \right)^{n_s-1} + P_p \exp \left[- \frac{(N_k - N_p)^2}{2\sigma_p^2} \right], \quad (4.4)$$

where $N_k = \ln(a(k)/a_{\text{end}})$ is the number of e-folds before the end of inflation when the mode k exits the horizon such that $N_p = \ln(a(k_p)/a_{\text{end}})$ and we consider $\sigma_p = 3$.

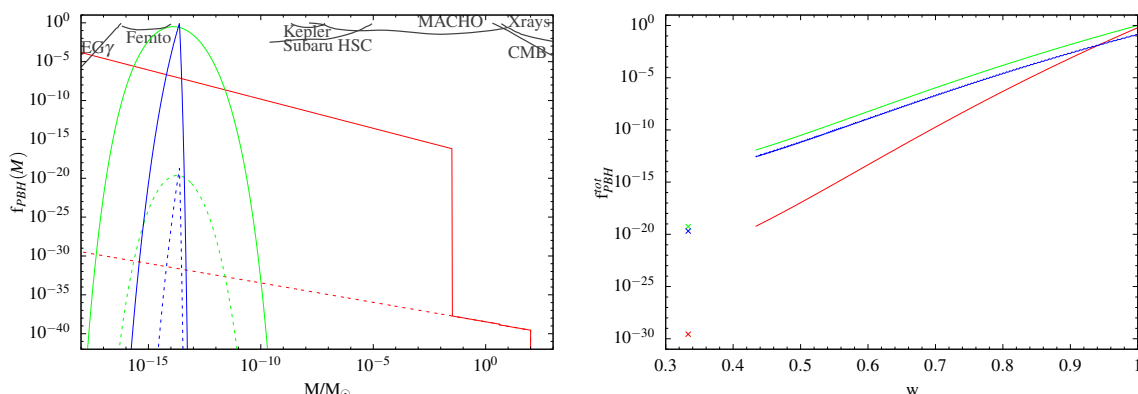


Figure 3. *Left panel:* Abundance of PBH for scale invariant power spectrum (red), for broken power law power spectrum (blue) and for gaussian power spectrum (green) for PBH formation in a pure radiation dominated epoch (dashed lines) and in a kination epoch before radiation domination (solid lines). Constraints on the PBH mass spectrum from different astrophysical and cosmological observations are shown in grey lines. *Right panel:* Total abundance of PBH (solid lines) as a function of equation of state w of an arbitrary epoch of scalar domination before radiation epoch, whereas crosses mark total abundance for OBH formation in a pure radiation epoch for the three different types of power spectra. The peak scale here is $k_p = 6 \times 10^{12} \text{ Mpc}^{-1}$ to have maximum power at the frequency $f = 10^{-2} \text{ Hz}$ where LISA proposes to have the best sensitivity.

For all three power spectra, the first term represents a red-tilted power spectrum at the CMB relevant scales, as constrained by Planck [2], with $A_s = 2.1 \times 10^{-9}$, $n_s = 0.9649$ and $k_* = 0.002 \text{ Mpc}^{-1}$. The second part of $P_\zeta(k)$, which reaches maximum amplitude at

$k = k_p$ for the Broken power law and Gaussian power spectrum, is relevant for leading to PBH formation of considerable abundance. The peak scale k_p shifts the features in the power spectrum along the mass of PBH whereas, theoretically, k_p is related to the dynamics of the underlying inflation model⁵.

The peak mode $k_p = 2 \times 10^6 \text{ Mpc}^{-1}$ is relevant for formation of solar mass PBH, which is explored in [44] for PBH formation in a radiation epoch. However, in this paper we explore the implications of $k_p = 2 \times 10^6 \text{ Mpc}^{-1}$ for PBH formed in an early kination epoch. Fig. 2 shows the mass spectrum for PBH for the scale-invariant (red), broken power law (blue) and Gaussian (green) power spectra with respect to several astrophysical and cosmological constraints (grey solid lines). This figure clearly points to a higher abundance $f_{\text{PBH}}(M)$ for PBH formation in an early kination epoch (solid lines) than formation in a radiation epoch (dashed lines). The right panel of the same figure shows the variation of the total PBH abundance $f_{\text{PBH}}^{\text{tot}}$ as a function of a general SD e.o.s. w in solid lines for three different power spectra, in comparison with PBH formation in a radiation epoch (represented by stars in the plot), which shows a gain in total abundance for the SD scenario as well and the gain increases as one moves farther away from $w = 1/3$. Here, we have considered $T_1 \simeq 10 \text{ MeV}$ that corresponds to PBH of a few solar mass in a radiation epoch. Therefore, with $k_p = 2 \times 10^6 \text{ Mpc}^{-1}$ the feature of the primordial power spectra spans through some part of the radiation epoch after SD as well. Thus, the mass spectrum in the left panel of Fig. 2 makes a transition from large abundance (solid lines) in a kination epoch to small abundance (dashed lines) in a radiation epoch at $M = M(T_1)$. Evidently, such a kination epoch is not helpful to have larger abundance for PBHs with $M \ll M_\odot$, but an such extremely massive PBHs can be formed at later epochs via merging of two or more solar or subsolar mass PBHs.

The same analysis has been carried out for $k_p = 6 \times 10^{12} \text{ Mpc}^{-1}$ corresponding to the frequency $f \simeq 0.01 \text{ Hz}$ which is the maximum sensitivity region for future LISA mission. As we derive the prediction for GW in presence of such early SD epochs in later sections, with $k_p = 6 \times 10^{12} \text{ Mpc}^{-1}$ we determine the amplitude of the curvature power spectrum required for a considerable abundance of PBHs of relevant masses around $10^{-17} M_\odot < M < 10^{-10} M_\odot$ for the Gaussian power spectrum and $10^{-16} M_\odot < M < 10^{-13} M_\odot$ for the broken power law power spectrum⁶. In this case, the transition to RD is taken to be at $T_1 = 100 \text{ MeV}$. Left panel of fig. 2 shows the mass spectrum for PBH for the three different power spectra and clearly points to a gain in abundance for an early kination epoch. The right panel in fig. 2 shows the variation of the total PBH abundance $f_{\text{PBH}}^{\text{tot}}$ as a function of w which signify a gain in total PBH abundance for $w > 1/3$ over radiation epoch $w = 1/3$.

The lower requirement for the amplitude of primordial power P_p is shown in the Table 1 which shows a significant improvement for $w = 1$ epoch with respect to the radiation epoch, specifically for the case $k_p = 6 \times 10^{12} \text{ Mpc}^{-1}$.

5 Modification of the Gravitational Wave spectra

Stochastic background of GW arise inevitably from the primordial tensor fluctuations given a model of inflation. Standard single field slow roll inflation models lead to the tensor power

⁵As an example, modifying k_p for the Gaussian power spectrum for an waterfall-hybrid inflation model would mean changing the starting point of the mild waterfall phase. Detailed discussion on the exact implication for inflation models in beyond the scope of this paper.

⁶Interestingly, this mass range includes the small mass window where it is still allowed by observations to achieve totality of DM from PBHs.

Table 1. Comparison of required amplitude of curvature power spectra for a SD epoch with $w = 1$ and for a radiation epoch to achieve a percent level abundance of DM.

k_p		Scale-inv P_p	Broken Power Law P_p	Gaussian P_p
$2 \times 10^6 \text{ Mpc}^{-1}$	$w = 1/3$	0.021	0.0275	0.025
$2 \times 10^6 \text{ Mpc}^{-1}$	$w = 1$	0.0048	0.015	0.0129
$6 \times 10^{12} \text{ Mpc}^{-1}$	$w = 1/3$	0.013	0.016	0.0163
$6 \times 10^{12} \text{ Mpc}^{-1}$	$w = 1$	0.0048	0.0069	0.0067

spectrum with a slight blue-tilt n_t , which has a lower bound from the observed tensor to scalar ratio $r < 0.067$ and the single field consistency relation $r = -8n_t$. The evolution of the primordial tensor fluctuations is source-free in the first order of perturbation theory. The energy density of GW today is determined as

$$\Omega_{\text{GW},0}(k) = \frac{k^2 \Delta_h^2(\eta_0, k)}{12a_0^2 H_0^2}, \quad (5.1)$$

where $\Delta_h^2(\eta_0, k) = \frac{2k^2}{\pi^2} |h_k(\eta_0)|^2$ is the tensor power spectrum today. The superhorizon tensor modes h_k^{inf} re-enter the Hubble radius at post-inflationary epochs and evolve through transfer function as $h_k(\eta_0) = h_k^{\text{inf}} \times T(k, \eta_0)$.

The transfer function $T(k, \eta_0)$ depends on the evolution of the background from the time of horizon re-entry of a mode k until the time of observation η_0 . For standard cosmology where the modes re-enter during radiation domination, the transfer function gives a constant growth for all modes k since the GW grows in the same way as the background ($\sim a^0$) in a radiation epoch. However, in alternate cosmological histories with an additional SD epoch, the transfer function behaves differently owing to the departure of w from $w = 1/3$ and the relative growth of GW is $\sim a^{4-3(1+w)}$.

5.1 First order perturbation theory

In the first order of perturbations, after horizon re-entry, the evolution of the source free tensor fluctuations depend on the e.o.s. w , the temperature of transition from SD to radiation: T_1 . The primordial tensor perturbations depend on the scale of inflation H_{inf} . Tracking the growth of GW from the first order tensor fluctuations from horizon re-entry until today, the GW energy density is [47]:

$$\Omega_{\text{GW},0}^{(1)}(k) = \frac{\Omega_{\text{rad},0}}{12\pi^2} \left(\frac{g_{*,k}}{g_{s,k}} \right) \left(\frac{g_{s,0}}{g_{s,k}} \right)^{4/3} \left(\frac{H_{\text{inf}}}{M_{\text{Pl}}} \right)^2 \frac{\Gamma^2(\alpha + 1/2)}{2^{2(1-\alpha)} \alpha^2 \Gamma^2(3/2)} \mathcal{W}(\kappa) \kappa^{2(1-\alpha)}, \quad (5.2)$$

where $\alpha = \frac{2}{1+3w}$ and

$$\mathcal{W}(\kappa) = \frac{\pi\alpha}{2\kappa} \left[\left(\kappa J_{\alpha+1/2}(\kappa) - J_{\alpha-1/2}(\kappa) \right)^2 + \kappa^2 J_{\alpha-1/2}^2(\kappa) \right]. \quad (5.3)$$

The resulting GW for an early kination epoch $w = 1$ for $T_1 = 490 \text{ GeV}$ is shown in Fig. 4. The bounds on GW from LIGO O1, O2 and O5 runs (red curves) and future LISA (purple curve) constrain the amplitude of GW produced in such an early kination epoch. CMB puts a bound on the GW energy density fraction as GW contribute to the radiation energy density.

If GWs are overproduced, they will affect the universe expansion rate during CMB decoupling, which may not be allowed from the constraint on the extra radiation component obtained from CMB. For the homogeneous initial condition of GW, CMB put an upper bound [57–60] on fraction of GW energy density as: $\Omega_{\text{GW}} h^2 \leq 2 \times 10^{-7}$ which is shown by the magenta dashed line. Particularly, LIGO O1 bound (top red curve) signifies that if there is an early kination epoch after inflation until $T_1 = 490$ GeV then the scale of inflation is below $H_{\text{inf}} \simeq 10^{13}$ GeV. Here, for simplicity, we have considered a scale-independent primordial tensor power spectrum, i.e., $n_t \simeq 0$.

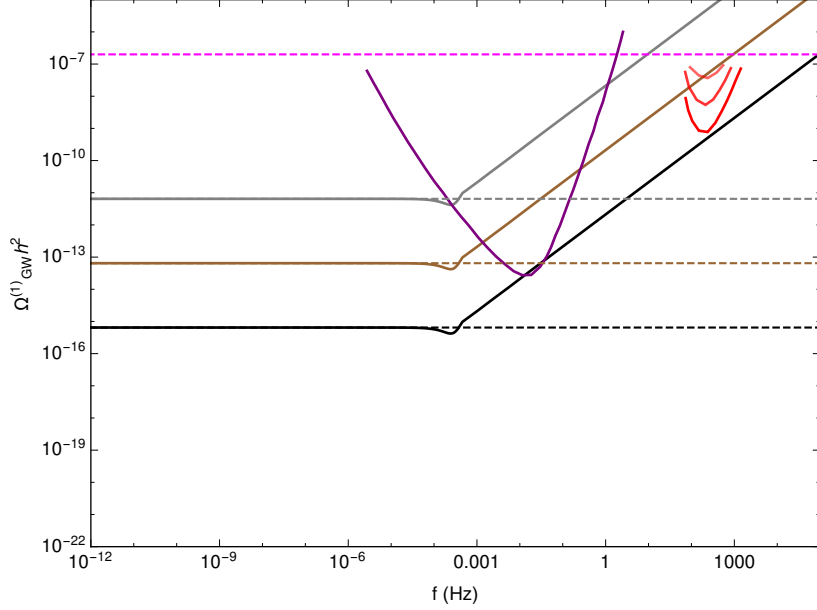


Figure 4. GW spectrum arising in the first order of perturbation theory for an early kination epoch $w = 1$ with $T_1 = 490$ GeV for $H_{\text{inf}} = 10^{12}$, 10^{13} and 10^{14} GeV for black, brown and grey curves respectively. Corresponding evolutions in a pure radiation epoch are shown by dashed black, brown and grey curves for respective cases. Bounds from CMB, LIGO and LISA are shown in magenta, red and purple lines respectively.

5.2 Second order perturbation theory

We have closely followed [61] to calculate the second order GW spectrum induced from the first order scalar perturbations. Evolution of second order gravitational wave amplitude h is given as

$$h_k'' + 2\mathcal{H}h_k' + k^2 h_k = \mathcal{S}(\mathbf{k}, \eta), \quad (5.4)$$

where the source term $\mathcal{S}(\mathbf{k}, \eta)$ is

$$\mathcal{S}(\mathbf{k}, \eta) = \int d^3\mathbf{p} p^2 [1 - \mu^2] f(\mathbf{k}, \mathbf{p}, \eta) \psi_{\mathbf{k}-\mathbf{p}} \psi_{\mathbf{p}}. \quad (5.5)$$

In this expression, $\psi_{\mathbf{p}}$ is the primordial scalar perturbation and $\mu = \frac{\mathbf{k} \cdot \mathbf{p}}{kp}$ with $f(\mathbf{k}, \mathbf{p}, \eta)$ given as:

$$f(\mathbf{k}, \mathbf{p}, \eta) = \frac{8}{3(1+w)} [(5+3w)\Phi(|\mathbf{k}-\mathbf{p}|\eta)\Phi(|\mathbf{p}|\eta) + 2(2\eta\Phi(|\mathbf{k}-\mathbf{p}|\eta) + \eta^2\Phi'(|\mathbf{k}-\mathbf{p}|\eta))\Phi'(|\mathbf{p}|\eta)]. \quad (5.6)$$

Where $\Phi(|\mathbf{p}|\eta)$ is the first order scalar transfer function, which is related to the Bardeen potential $\Phi_{\mathbf{p}}(\eta)$ and primordial fluctuations $\psi_{\mathbf{p}}$ as:

$$\Phi_{\mathbf{p}}(\eta) = \Phi(p\eta) \psi_{\mathbf{p}}. \quad (5.7)$$

Now, in order to calculate the evolution of source term we need to calculate the first order scalar transfer function $\Phi(p\eta)$. In the appendix A, we have derived the expression for $\Phi(p\eta)$ to be

$$\Phi(p\eta) = \begin{cases} \frac{1}{1+(p\eta)^{3/2}} & \eta < \eta_{\Gamma 1} \\ \frac{1}{1+(p\eta)^2} & \eta_{\Gamma 1} < \eta < \eta_{\text{eq}} \\ \frac{1}{1+(p\eta_{\text{eq}})^2} & \eta > \eta_{\text{eq}} \end{cases} \quad (5.8)$$

We are working under the approximation that GW are generated instantaneously as the

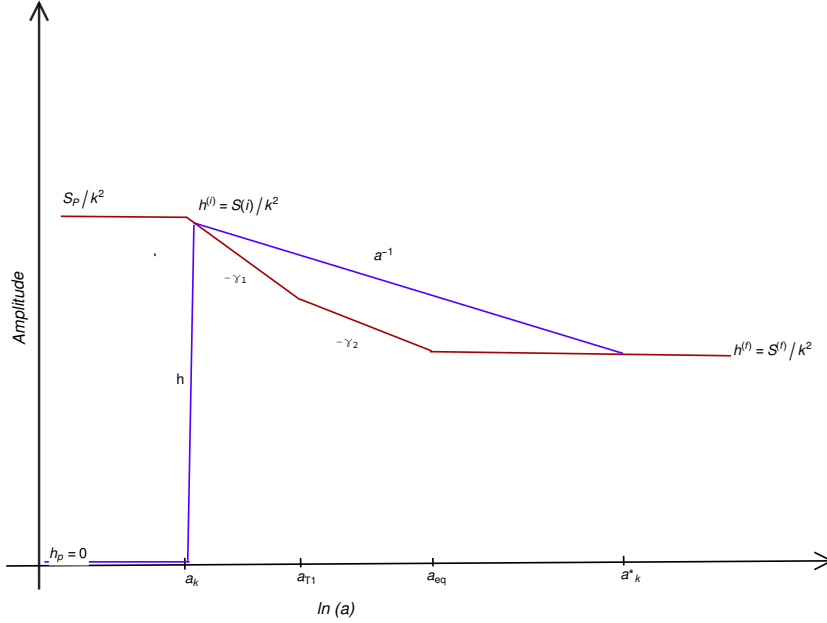


Figure 5. Evolution of scalar source and induced gravitational waves throughout different epochs after horizon re-entry. The source evolves as $a^{-\gamma_1}$ and $a^{-\gamma_2}$ in the kination and radiation epoch respectively and becomes constant at the beginning of matter domination. The induced tensor fluctuations evolve as a^{-1} during kination and radiation era and settle down at some later epoch (matter domination) at the constant value set by the source term. The modes relevant to our analysis correspond to very high frequencies, and therefore they have not yet settled down completely at the constant value of the source term.

primordial curvature perturbations of a particular mode enter the horizon. After that, the evolution of that mode is governed by the transfer function. Therefore second order tensor transfer function $t(k, \eta)$ is defined as

$$h_k(\eta) = t(k, \eta) h_k^{(i)}, \quad (5.9)$$

where $h_k^{(i)}$ is the GW amplitude at the horizon entry. At the horizon entry, we can neglect the time derivative terms in (5.4) to calculate the $h_k^{(i)}$ so that

$$h_k^{(i)} \sim \frac{1}{k^2} \mathcal{S}^{(i)}. \quad (5.10)$$

The power spectrum for any mode at the time of horizon crossing is defined as

$$P_h^{(i)}(k, \eta_i(k)) = \frac{k^3}{2\pi^2} \langle (h_k^{(i)})^2 \rangle, \quad (5.11)$$

where $\eta_i(k)$ is the time when mode k enters the horizon. After horizon entry, the mode evolves according to the transfer function, such that the second order power spectrum at any time can be written as:

$$P_h(k, \eta) = t(k, \eta)^2 P_h^{(i)}(k, \eta_i). \quad (5.12)$$

Now the expression for power spectrum at horizon crossing $P_h^{(i)}(k, \eta_i)$ can be derived using the Eq.s (5.5), (5.10) and (5.11). After some straightforward algebra, we arrive at

$$P_h^{(i)}(k) = \frac{k^3}{2\pi^2} \langle (h_k^{(i)})^2 \rangle \sim \frac{1}{2\pi^2 k} \int d^3 \mathbf{p} p^4 (1 - \mu^2)^2 \Phi^2(p\eta_i) \Phi^2(|\mathbf{k} - \mathbf{p}|\eta_i) \frac{P(p)}{p^3} \frac{P(|\mathbf{k} - \mathbf{p}|)}{|\mathbf{k} - \mathbf{p}|^3}. \quad (5.13)$$

Where $P(p)$ is the primordial scalar power spectrum. In this work we have used two different scalar power spectra, as explained in section 4, to calculate second order the tensor power spectra.

5.2.1 Tensor Transfer Function

Second order tensor transfer function depends on the evolution of the source term \mathcal{S} . In Fig. 5 we have shown how the evolution of source term and the amplitude of GW changes if we have an extra period of stiff domination. Now let us consider a mode $k = a_k H$, which enters the horizon during SD period. At horizon entry, the GW amplitude immediately becomes equal to the source term as given in Eq. (5.10). If the source term decays as a^{γ_1} during the SD era and as a^{γ_2} during radiation dominated era, then

$$\frac{\mathcal{S}^{(f)}}{\mathcal{S}^{(i)}} = \left(\frac{a_k}{a_{T1}} \right)^{\gamma_1} \left(\frac{a_{T1}}{a_{\text{eq}}} \right)^{\gamma_2}, \quad (5.14)$$

where a_{T1} is the scale factor at the time when SD ends. It was show in the ref. [61] that source term, $\mathcal{S} \approx \frac{1}{\eta^2} \frac{1}{(k\eta)^2} \propto \frac{1}{a^4}$ in a radiation epoch. We assume that source term will decay faster in SD than that in radiation era *i.e.* $\gamma_2 < \gamma_1$. On the other hand GW amplitude h just redshifts as a^{-1} till the time it becomes equal to source term at time a_k^* . Therefore, we have

$$\frac{h^{(f)}}{h^{(i)}} = \frac{a_k}{a_k^*} \approx \frac{\mathcal{S}^{(f)}}{\mathcal{S}^{(i)}} = \left(\frac{a_k}{a_{T1}} \right)^{\gamma_1} \left(\frac{a_{T1}}{a_{\text{eq}}} \right)^{\gamma_2}, \quad (5.15)$$

Now let us define a sufficiently large scale k_c for a fixed time η , such that modes with $k > k_c$ have never settled down by the time η , they just keep on redshifting as a^{-1} . Thus,

$$k_c(\eta) = \left(\frac{a(\eta)}{a_{T1}} \right)^{1/(\gamma_1-1)} \frac{k_{\text{eq}}^{\gamma_1-1}}{k_{T1}^{\gamma_1-1}} \frac{k_{T1}^{\gamma_2-\gamma_1-1}}{k_{\text{eq}}^{\gamma_2-\gamma_1-1}}. \quad (5.16)$$

Where k_{T1} is the scale corresponding to time a_{T1} . Now if there is no SD era, then feeding in $\gamma_1 = \gamma_2$ and $k_{T1} = k_{\text{eq}}$ in this relation gives back the result in radiation era obtained in [61]. Now for the modes with $k > k_c$, transfer function is given as

$$t(k, \eta) = \frac{a_k}{a(\eta)} = \left(\frac{k_{T1}}{k}\right)^{1/2} \frac{k_{\text{eq}}}{k_{T1}} a_{\text{eq}}, \quad k > k_c(\eta). \quad (5.17)$$

However, for the modes with $k_{T1} < k < k_c(\eta)$, transfer function is given as

$$t(k, \eta) = \left(\frac{k_{T1}}{k}\right)^{\gamma_1/2} \left(\frac{k_{\text{eq}}}{k_{T1}}\right)^{\gamma_2}, \quad k_{T1} < k < k_c(\eta). \quad (5.18)$$

Now combining these results with the transfer functions obtained in [61], we get the full second order transfer function for all the modes:

$$t(k, \eta) = \begin{cases} 1 & k < k_{\text{eq}} \\ \left(\frac{k}{k_{\text{eq}}}\right)^{-\gamma_2} & k_{\text{eq}} < k < k_c(\eta) \\ \left(\frac{k_{T1}}{k}\right)^{\gamma_1/2} \left(\frac{k_{\text{eq}}}{k_{T1}}\right)^{\gamma_2} & k_{T1} < k < k_c(\eta) \\ \left(\frac{k_{T1}}{k}\right)^{1/2} \frac{k_{\text{eq}}}{k_{T1}} a_{\text{eq}} & k > k_c(\eta) \end{cases} \quad (5.19)$$

We now have all the necessary quantities to calculate the initial tensor power spectrum as well as the final GW spectrum. For the purpose of analysis relevant for this paper, we are working in the regime $k > k_{T1}$, therefore using the expression for $\Phi(k\eta)$ from Eq. (5.8) valid in this regime, we can rewrite the expression for $P_h^{(i)}(k)$ as

$$P_h^{(i)}(k) \simeq \frac{1}{\pi k} \int_0^\infty dp \int_{-1}^1 d\mu \frac{p^3 (1 - \mu^2)^2 P(p) P(\sqrt{|k^2 + p^2 - 2\mu kp|})}{\left(1 + \left(\frac{p}{k}\right)^{3/2}\right)^2 \left(1 + \left(\frac{|k^2 + p^2 - 2\mu kp|^{1/2}}{k}\right)^{3/2}\right)^2 (|k^2 + p^2 - 2\mu kp|)^{3/2}} \quad (5.20)$$

We will solve this equation for two different primordial scalar power spectra. Now, the fraction of second order GW energy density today, $\Omega_{\text{GW},0}^{(2)}$ is then given by

$$\Omega_{\text{GW},0}^{(2)} = \frac{a_0 k^2}{a_{\text{eq}} k_{\text{eq}}^2} t^2(k, \eta_0) P_h^{(i)}(k). \quad (5.21)$$

5.2.2 Second order GW spectrum for Gaussian Power spectrum

First, we use the Gaussian power spectrum given by Eq. (4.4) to calculate the tensor power spectrum at horizon crossing. We have fixed $P_p = 0.0067$, $\sigma_p = 3$ and pivot scale $k_p = 6 \times 10^{12} \text{Mpc}^{-1}$. We have solved the integral given by Eq. (5.20) numerically for the k values in between $10^{-3} k_p$ and $10^3 k_p$. We also find that all the modes relevant to this analysis are greater than the critical scale (k_c). Finally, we calculate the fraction of GW energy density at present epoch $\Omega_{\text{GW},0}^{(2)}$. Obtained GW spectrum is shown in the fig. 5.2.1. It can be seen from the fig. 5.2.1 that it peaks at $k = 2 \times 10^{14} \text{Mpc}^{-1}$ and its peak value is 8.4×10^{-8} .

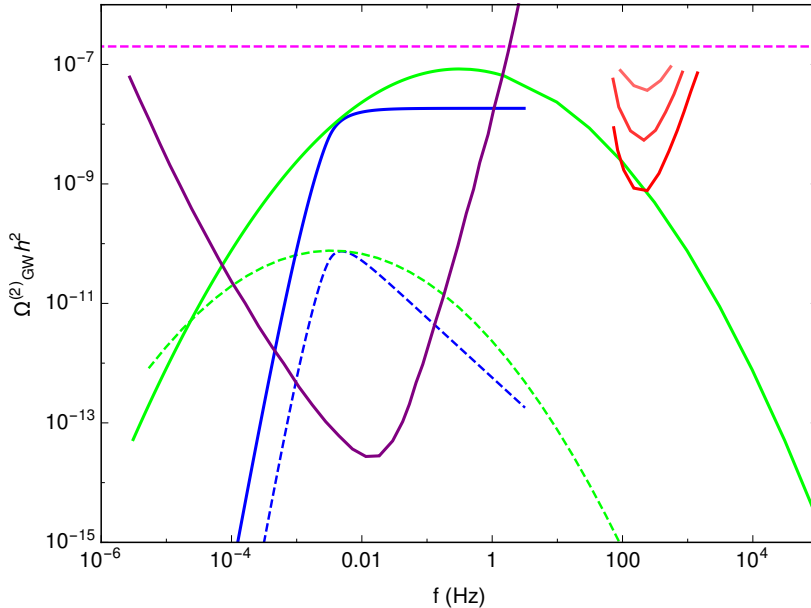


Figure 6. Second order GW spectrum for the Gaussian primordial power spectrum (green curve) and broken power law power spectrum (blue curve) for the cases when relevant modes enter the horizon in a kination epoch (solid lines) and in a radiation epoch (dashed line). The spectrum in the kination epoch is enhanced for both the cases over that in the radiation epoch. Bounds from CMB, LIGO and LISA are shown in magenta, red and purple lines respectively.

5.2.3 Second order GW spectrum for Broken Power spectrum

In order to solve for initial tensor power spectrum with broken power law scalar power spectrum, we put $x = p/k$ and use the broken power law spectrum given by Eq. (4.3). Therefore the expression for $P_h^{(i)}(k)$ is now given as

$$\begin{aligned}
 P_h^{(i)}(k) \simeq & \frac{2\mathcal{P}_p^2}{\pi} \left(\frac{k}{k_p}\right)^{2m} \int_0^{k_p/k} dx \int_{-1}^1 d\mu \frac{(1-\mu^2)^2(1+x^2-2x\mu)^{\frac{m-3}{2}} x^{m+3}}{(1+(\sqrt{1+x^2-2x\mu})^{3/2})^2(1+x^{3/2})^2} \\
 & + \frac{2\mathcal{P}_p^2}{\pi} \left(\frac{k}{k_p}\right)^{-2n} \int_{k_p/k}^\infty dx \int_{-1}^1 d\mu \frac{(1-\mu^2)^2(1+x^2-2x\mu)^{\frac{-n-3}{2}} x^{-n+3}}{(1+(\sqrt{1+x^2-2x\mu})^{3/2})^2(1+x^{3/2})^2}
 \end{aligned} \tag{5.22}$$

We have fixed $P_p = 0.0069$, $m = 3$, $n = 0.5$ and pivot scale $k_p = 6 \times 10^{12} \text{Mpc}^{-1}$. We then numerically solve these integrals for the k values lying in the range $[10^{-3}k_p, 10^3k_p]$. Using this and the appropriate transfer function, we calculate the $\Omega_{\text{GW},0}^{(2)}$, which is plotted against frequency in fig. 5.2.1. Again, it is evident from the Fig. 5.2.1 that it reaches the maximum value at $k = 6 \times 10^{12}$ and then becomes constant.

6 Discussion and summary

PBH formed in the early universe can be considered as a probe for the smaller scales of inflation as well as for pre-BBN cosmology in alternate settings. In this paper, given a primordial power spectrum with a rise in amplitude for the smaller scales, we have discussed the effect of an alternate pre-BBN cosmological history in the abundance of PBH and on the

amplitude of first and second order GW. Sec. 3 discusses the modification of the PBH mass spectrum $f_{\text{PBH}}(M)$ and the total PBH abundance $f_{\text{PBH}}^{\text{tot}}$ in an arbitrary pre-BBN SD epoch and comments on the possible gain in abundance in contrast with PBH formed in a radiation era. The analysis in Sec. 4 explains that the requirement of the amplitude of primordial curvature power spectrum $P_{\zeta}(k)$ is lower for PBH formation in a SD epoch with $1/3 < w < 1$ than in a radiation epoch. Exact calculations for $f_{\text{PBH}}^{\text{tot}} \sim 10\%$ are quoted in Table 1 which show that a kination epoch ($w = 1$) requires almost half of the amplitude of $P_{\zeta}(k)$ at the peak at $k = k_p$ in contrast with reaching the same abundance in RD. Exact mass spectra are shown for three different features of the rise in amplitude of $P_{\zeta}(k)$ in Fig. 2 and Fig. 3 for two different positions of the peak at $k_p = 2 \times 10^6 \text{ Mpc}^{-1}$ and $k_p = 6 \times 10^{12} \text{ Mpc}^{-1}$ respectively.

In Sec. 5, we have analysed the effect of such an early SD epoch on the resulting GW spectrum. The first order GW spectrum calculated in subsection 5.1 has an enhancement for the modes that enter the horizon during SD epoch due to modification in the transfer function in this epoch. The final $\Omega_{\text{GW},0}^{(1)}(k)$ depends on w , T_1 and H_{inf} . Here, for an early kination epoch $w = 1$ we have considered a particular frequency $f(T_1) \simeq 10^{-4}$ where this epoch end and radiation starts to dominate at $T_1 = 490 \text{ GeV}$. The T_1 considered to calculate GW spectra in Sec. 5 is different than that considered while calculating PBH abundance in Sec. 4, for the reason that moving T_1 towards T_{BBN} enhances the GW power spectra even more which can overshoot the bound from CMB. However, a high value of T_1 leads to a smaller value of the last term in Eq. (3.16) resulting in a smaller gain in the kination epoch as compared to radiation epoch. Then, to reach desirable PBH abundance, the power requirement may be little higher than what is quoted in Table 1 for $w = 1$, however, it will still be smaller than that required for $w = 1/3$.

Present and future GW interferometers such as aLIGO and LISA will constrain the scale of inflation. Fig. 4 shows that non-observation of primordial GW signal in LIGO O1 constrains $H_{\text{inf}} \leq 10^{13} \text{ GeV}$, which is consistent with the current upper bound on the tensor-to-scalar ratio $r < 0.067$ from Planck [2]. Large primordial curvature perturbations at small scales that are relevant for PBH formation can source second order GW. In case of an early SD epoch, the second order GW profile is calculated in subsection 5.2 for the broken power law and Gaussian primordial spectrum for frequencies that are relevant to the future sensitivity range of LISA corresponding to $k_p = 6 \times 10^{12} \text{ Mpc}^{-1}$. We found that for the same primordial spectra, the second order GW amplitude is enhanced in a kination epoch as compared to a pure radiation epoch. Upcoming LISA observation can therefore constrain the equation of state of a possible early SD epoch given the small scale primordial spectrum.

If primordial curvature perturbations have large amplitude at such small scales then any observed GW spectrum in LISA can have contributions from all orders in perturbation theory. Although in our case, the orders of the first and second order GW spectrum are quite different considering $H_{\text{inf}} \sim 10^{13} \text{ GeV}$, degeneracies in the amplitude of GW spectrum originating at different orders of perturbation theory may arise for other cases with a different $P_{\zeta}(k)$ or different w, T_1 . A possible way to break the degeneracy in the contribution from first and second order is that the first order GW spectrum will not depend on the feature of $P_{\zeta}(k)$, whereas the second order GW spectrum tracks the profile of $P_{\zeta}(k)$.

The effects of an early kination epoch on PBH formation and GW discussed in this paper points to an interesting path to phenomenology by simultaneously considering the observational constraints on the PBH mass spectrum and observational constraints on the amplitude and feature of the GW from future GW surveys. This paper focuses on the proposed sensitivity and relevant frequency range for future LISA mission, whereas similar analysis

can be carried out for present and future PTA observations for GW spectrum, where the relevant frequency range is $f \sim 10^{-8}$ Hz, which corresponds to near solar mass PBH. With the proposed improvement in precision for the astrophysical and cosmological experiments constraining PBH abundance and with the proposed high sensitivity of future GW missions such as LISA and aLIGO, DECIGO and PTA, a rich phenomenological understanding of the pre-BBN epoch is expected and intended. Moreover, the theories leading to a non-standard pre-BBN epoch such as quintessential inflation leading to an early kination epoch can be constrained with such a phenomenological analysis.

The exact implications of the inflationary power spectrum for PBH formation in a kination epoch can be interpreted in terms of parameters and field values of the underlying model of inflation. An early SD epoch, particularly a pre-BBN kination epoch may also have interesting predictions for the spin of the PBH formed in this epoch. The merger rate for PBH formed in such an epoch [62] can also be calculated. We hope to explore these aspects of non-standard pre-BBN cosmology in future.

References

- [1] N. Aghanim *et al.* [Planck Collaboration], arXiv:1807.06209 [astro-ph.CO].
- [2] Y. Akrami *et al.* [Planck Collaboration], arXiv:1807.06211 [astro-ph.CO].
- [3] S. Hawking, Mon. Not. Roy. Astron. Soc. **152**, 75 (1971).
- [4] B. J. Carr and S. W. Hawking, Mon. Not. Roy. Astron. Soc. **168**, 399 (1974).
- [5] B. J. Carr, Astrophys. J. **201**, 1 (1975). doi:10.1086/153853
- [6] B. P. Abbott *et al.* [LIGO Scientific and Virgo Collaborations], Phys. Rev. Lett. **116**, no. 6, 061102 (2016) doi:10.1103/PhysRevLett.116.061102 [arXiv:1602.03837 [gr-qc]].
- [7] B. P. Abbott *et al.* [LIGO Scientific and Virgo Collaborations], Phys. Rev. Lett. **116**, no. 24, 241103 (2016) doi:10.1103/PhysRevLett.116.241103 [arXiv:1606.04855 [gr-qc]].
- [8] B. P. Abbott *et al.* [LIGO Scientific and Virgo Collaborations], Phys. Rev. X **6**, no. 4, 041015 (2016) Erratum: [Phys. Rev. X **8**, no. 3, 039903 (2018)] doi:10.1103/PhysRevX.6.041015, 10.1103/PhysRevX.8.039903 [arXiv:1606.04856 [gr-qc]].
- [9] B. P. Abbott *et al.* [LIGO Scientific and Virgo Collaborations], Annalen Phys. **529**, no. 1-2, 1600209 (2017) doi:10.1002/andp.201600209 [arXiv:1608.01940 [gr-qc]].
- [10] B. P. Abbott *et al.* [LIGO Scientific and VIRGO Collaborations], Phys. Rev. Lett. **118**, no. 22, 221101 (2017) Erratum: [Phys. Rev. Lett. **121**, no. 12, 129901 (2018)] doi:10.1103/PhysRevLett.118.221101, 10.1103/PhysRevLett.121.129901 [arXiv:1706.01812 [gr-qc]].
- [11] B. P. Abbott *et al.* [LIGO Scientific and Virgo Collaborations], Astrophys. J. **851**, no. 2, L35 (2017) doi:10.3847/2041-8213/aa9f0c [arXiv:1711.05578 [astro-ph.HE]].
- [12] B. P. Abbott *et al.* [LIGO Scientific and Virgo Collaborations], Phys. Rev. Lett. **119**, no. 14, 141101 (2017) doi:10.1103/PhysRevLett.119.141101 [arXiv:1709.09660 [gr-qc]].
- [13] B. J. Carr, K. Kohri, Y. Sendouda and J. Yokoyama, Phys. Rev. D **81**, 104019 (2010) doi:10.1103/PhysRevD.81.104019 [arXiv:0912.5297 [astro-ph.CO]].
- [14] A. Barnacka, J. F. Glicenstein and R. Moderski, Phys. Rev. D **86**, 043001 (2012) doi:10.1103/PhysRevD.86.043001 [arXiv:1204.2056 [astro-ph.CO]].
- [15] P. Tisserand *et al.* [EROS-2 Collaboration], Astron. Astrophys. **469**, 387 (2007) doi:10.1051/0004-6361:20066017 [astro-ph/0607207].

- [16] R. A. Allsman *et al.* [Macho Collaboration], *Astrophys. J.* **550**, L169 (2001) doi:10.1086/319636 [astro-ph/0011506].
- [17] Y. Inoue and A. Kusenko, *JCAP* **1710**, 034 (2017) doi:10.1088/1475-7516/2017/10/034 [arXiv:1705.00791 [astro-ph.CO]].
- [18] D. Gaggero, G. Bertone, F. Calore, R. M. T. Connors, M. Lovell, S. Markoff and E. Storm, *Phys. Rev. Lett.* **118**, no. 24, 241101 (2017) doi:10.1103/PhysRevLett.118.241101 [arXiv:1612.00457 [astro-ph.HE]].
- [19] H. Niikura *et al.*, *Nat. Astron.* **3**, no. 6, 524 (2019) doi:10.1038/s41550-019-0723-1 [arXiv:1701.02151 [astro-ph.CO]].
- [20] H. Motohashi and W. Hu, *Phys. Rev. D* **96**, no. 6, 063503 (2017) doi:10.1103/PhysRevD.96.063503 [arXiv:1706.06784 [astro-ph.CO]].
- [21] A. Linde, S. Mooij and E. Pajer, *Phys. Rev. D* **87**, no. 10, 103506 (2013) doi:10.1103/PhysRevD.87.103506 [arXiv:1212.1693 [hep-th]].
- [22] E. Bugaev and P. Klimai, *Phys. Rev. D* **90**, no. 10, 103501 (2014) doi:10.1103/PhysRevD.90.103501 [arXiv:1312.7435 [astro-ph.CO]].
- [23] E. Erfani, *JCAP* **1604**, 020 (2016) doi:10.1088/1475-7516/2016/04/020 [arXiv:1511.08470 [astro-ph.CO]].
- [24] S. L. Cheng, W. Lee and K. W. Ng, *JHEP* **1702**, 008 (2017) doi:10.1007/JHEP02(2017)008 [arXiv:1606.00206 [astro-ph.CO]].
- [25] J. Garcia-Bellido, M. Peloso and C. Unal, *JCAP* **1612**, 031 (2016) doi:10.1088/1475-7516/2016/12/031 [arXiv:1610.03763 [astro-ph.CO]].
- [26] J. Garcia-Bellido, M. Peloso and C. Unal, *JCAP* **1709**, 013 (2017) doi:10.1088/1475-7516/2017/09/013 [arXiv:1707.02441 [astro-ph.CO]].
- [27] J. Garcia-Bellido and E. Ruiz Morales, *Phys. Dark Univ.* **18**, 47 (2017) doi:10.1016/j.dark.2017.09.007 [arXiv:1702.03901 [astro-ph.CO]].
- [28] J. M. Ezquiaga, J. Garcia-Bellido and E. Ruiz Morales, *Phys. Lett. B* **776**, 345 (2018) doi:10.1016/j.physletb.2017.11.039 [arXiv:1705.04861 [astro-ph.CO]].
- [29] F. Bezrukov, M. Pauly and J. Rubio, *JCAP* **1802**, 040 (2018) doi:10.1088/1475-7516/2018/02/040 [arXiv:1706.05007 [hep-ph]].
- [30] T. J. Gao and Z. K. Guo, *Phys. Rev. D* **98**, no. 6, 063526 (2018) doi:10.1103/PhysRevD.98.063526 [arXiv:1806.09320 [hep-ph]].
- [31] R. Arya, arXiv:1910.05238 [astro-ph.CO].
- [32] B. Carr, K. Dimopoulos, C. Owen and T. Tenkanen, *Phys. Rev. D* **97**, no. 12, 123535 (2018) doi:10.1103/PhysRevD.97.123535 [arXiv:1804.08639 [astro-ph.CO]].
- [33] T. Harada, C. M. Yoo, K. Kohri and K. I. Nakao, *Phys. Rev. D* **96**, no. 8, 083517 (2017) Erratum: [*Phys. Rev. D* **99**, no. 6, 069904 (2019)] doi:10.1103/PhysRevD.99.069904, 10.1103/PhysRevD.96.083517 [arXiv:1707.03595 [gr-qc]].
- [34] T. Matsubara, T. Terada, K. Kohri and S. Yokoyama, arXiv:1909.04053 [astro-ph.CO].
- [35] L. Alabidi, K. Kohri, M. Sasaki and Y. Sendouda, *JCAP* **1305**, 033 (2013) doi:10.1088/1475-7516/2013/05/033 [arXiv:1303.4519 [astro-ph.CO]].
- [36] T. Harada, C. M. Yoo, K. Kohri, K. i. Nakao and S. Jhingan, *Astrophys. J.* **833**, no. 1, 61 (2016) doi:10.3847/1538-4357/833/1/61 [arXiv:1609.01588 [astro-ph.CO]].
- [37] B. Carr, T. Tenkanen and V. Vaskonen, *Phys. Rev. D* **96**, no. 6, 063507 (2017) doi:10.1103/PhysRevD.96.063507 [arXiv:1706.03746 [astro-ph.CO]].

- [38] J. c. Hwang, H. Noh and J. O. Gong, *Astrophys. J.* **752**, 50 (2012)
doi:10.1088/0004-637X/752/1/50 [arXiv:1204.3345 [astro-ph.CO]].
- [39] L. Lentati *et al.*, *Mon. Not. Roy. Astron. Soc.* **453**, no. 3, 2576 (2015)
doi:10.1093/mnras/stv1538 [arXiv:1504.03692 [astro-ph.CO]].
- [40] Z. Arzoumanian *et al.* [NANOGrav Collaboration], *Astrophys. J.* **821**, no. 1, 13 (2016)
doi:10.3847/0004-637X/821/1/13 [arXiv:1508.03024 [astro-ph.GA]].
- [41] P. D. Lasky *et al.*, *Phys. Rev. X* **6**, no. 1, 011035 (2016) doi:10.1103/PhysRevX.6.011035
[arXiv:1511.05994 [astro-ph.CO]].
- [42] N. Bartolo *et al.*, *JCAP* **1612**, 026 (2016) doi:10.1088/1475-7516/2016/12/026
[arXiv:1610.06481 [astro-ph.CO]].
- [43] S. Clesse and J. Garcia-Bellido, *Phys. Rev. D* **92**, no. 2, 023524 (2015)
doi:10.1103/PhysRevD.92.023524 [arXiv:1501.07565 [astro-ph.CO]].
- [44] S. Clesse, J. Garcia-Bellido and S. Orani, arXiv:1812.11011 [astro-ph.CO].
- [45] C. Germani and T. Prokopec, *Phys. Dark Univ.* **18**, 6 (2017) doi:10.1016/j.dark.2017.09.001
[arXiv:1706.04226 [astro-ph.CO]].
- [46] A. Di Marco, G. Pradisi and P. Cabella, *Phys. Rev. D* **98**, no. 12, 123511 (2018)
doi:10.1103/PhysRevD.98.123511 [arXiv:1807.05916 [astro-ph.CO]].
- [47] D. G. Figueroa and E. H. Tanin, *JCAP* **1908**, 011 (2019) doi:10.1088/1475-7516/2019/08/011
[arXiv:1905.11960 [astro-ph.CO]].
- [48] P. J. E. Peebles and A. Vilenkin, *Phys. Rev. D* **59**, 063505 (1999)
doi:10.1103/PhysRevD.59.063505 [astro-ph/9810509].
- [49] S. Ahmad, A. De Felice, N. Jaman, S. Kuroyanagi and M. Sami, *Phys. Rev. D* **100**, no. 10,
103525 (2019) doi:10.1103/PhysRevD.100.103525 [arXiv:1908.03742 [gr-qc]].
- [50] S. Young, C. T. Byrnes and M. Sasaki, *JCAP* **1407**, 045 (2014)
doi:10.1088/1475-7516/2014/07/045 [arXiv:1405.7023 [gr-qc]].
- [51] T. Harada, C. M. Yoo and K. Kohri, *Phys. Rev. D* **88**, no. 8, 084051 (2013) Erratum: [*Phys.*
Rev. D **89**, no. 2, 029903 (2014)] doi:10.1103/PhysRevD.88.084051,
10.1103/PhysRevD.89.029903 [arXiv:1309.4201 [astro-ph.CO]].
- [52] A. Kalaja, N. Bellomo, N. Bartolo, D. Bertacca, S. Matarrese, I. Musco, A. Raccanelli and
L. Verde, *JCAP* **1910**, no. 10, 031 (2019) doi:10.1088/1475-7516/2019/10/031
[arXiv:1908.03596 [astro-ph.CO]].
- [53] H. Deng, J. Garriga and A. Vilenkin, *JCAP* **1704**, 050 (2017)
doi:10.1088/1475-7516/2017/04/050 [arXiv:1612.03753 [gr-qc]].
- [54] H. Deng and A. Vilenkin, *JCAP* **1712**, 044 (2017) doi:10.1088/1475-7516/2017/12/044
[arXiv:1710.02865 [gr-qc]].
- [55] E. Cotner and A. Kusenko, *Phys. Rev. D* **96**, no. 10, 103002 (2017)
doi:10.1103/PhysRevD.96.103002 [arXiv:1706.09003 [astro-ph.CO]].
- [56] E. Cotner and A. Kusenko, *Phys. Rev. Lett.* **119**, no. 3, 031103 (2017)
doi:10.1103/PhysRevLett.119.031103 [arXiv:1612.02529 [astro-ph.CO]].
- [57] C. Caprini and D. G. Figueroa, *Class. Quant. Grav.* **35**, no. 16, 163001 (2018)
doi:10.1088/1361-6382/aac608 [arXiv:1801.04268 [astro-ph.CO]].
- [58] K. M. Smith, W. Hu and M. Kaplinghat, *Phys. Rev. D* **74**, 123002 (2006)
doi:10.1103/PhysRevD.74.123002 [astro-ph/0607315].
- [59] I. Sendra and T. L. Smith, *Phys. Rev. D* **85**, 123002 (2012) doi:10.1103/PhysRevD.85.123002
[arXiv:1203.4232 [astro-ph.CO]].

- [60] L. Pagano, L. Salvati and A. Melchiorri, *Phys. Lett. B* **760**, 823 (2016)
doi:10.1016/j.physletb.2016.07.078 [arXiv:1508.02393 [astro-ph.CO]].
- [61] D. Baumann, P. J. Steinhardt, K. Takahashi and K. Ichiki, *Phys. Rev. D* **76**, 084019 (2007)
doi:10.1103/PhysRevD.76.084019 [hep-th/0703290].
- [62] V. Korol, I. Mandel, M. C. Miller, R. P. Church and M. B. Davies, arXiv:1911.03483
[astro-ph.HE].

A Transfer function for first-order scalar modes

In the absence of entropy perturbation, evolution of the $\Phi_{\mathbf{p}}$ in any epoch with equation of state parameter w , is governed by the following equation (see Eq.(B3) in [61]).

$$\Phi_{\mathbf{p}}'' + \frac{6(1+w)}{1+3w} \frac{1}{\eta} \Phi_{\mathbf{p}}' + wp^2 \Phi_{\mathbf{p}} = 0. \quad (\text{A.1})$$

Exact solution for this equation can be obtained in terms of Bessel function, which is given as

$$\Phi_{\mathbf{p}}(\eta) = y^{-\alpha} \left[C_1(p) J_\alpha(y) + C_2(p) Y_\alpha(y) \right], \quad (\text{A.2})$$

where $y \equiv \sqrt{w} p \eta$, $\alpha \equiv \frac{1}{2} \left(\frac{5+3w}{1+3w} \right)$, J_α and Y_α are Bessel functions of order α . For $w = 1$,

$$\Phi_{\mathbf{p}}(\eta) = \frac{1}{p\eta} \left[C_1(p) J_1(p\eta) + C_2(p) Y_1(p\eta) \right] \quad (\text{A.3})$$

We will drop the second term as this gives unphysical solution. This expression gives the primordial value of $\Phi_{\mathbf{p}}$ in the early time limit $y = \sqrt{w} p \eta \ll 1$

$$\lim_{y \rightarrow 0} \Phi_{\mathbf{p}}(\eta) = \frac{C_1(p)}{2} = \psi_{\mathbf{p}}, \quad (\text{A.4})$$

Now for the superhorizon modes ($p\eta \ll 1$)

$$\Phi(p\eta) = 1 + \mathcal{O}((p\eta)^2) \quad (\text{A.5})$$

and for the subhorizon modes ($p\eta > 1$)

$$\Phi(p\eta) \simeq \frac{1}{(p\eta)^{3/2}} \cos\left(\frac{3\pi}{2} - p\eta\right). \quad (\text{A.6})$$

This can be written as follows, which will be valid for both super and sub horizon modes

$$\Phi(p\eta) = \frac{1}{1 + (p\eta)^{3/2}}, \quad \eta < \eta_{\text{T1}}, \quad (\text{A.7})$$

where we have neglected the oscillation term. This can be compared with the expression for the first order scalar transfer function in [61] given as:

$$\Phi(p\eta) = \begin{cases} \frac{1}{1+p^2\eta^2} & \eta_{\text{T1}} < \eta < \eta_{\text{eq}} \\ \frac{1}{1+p^2\eta_{\text{eq}}^2} & \eta > \eta_{\text{eq}} \end{cases} \quad (\text{A.8})$$